ELSEVIER

Journal of Power Sources 114 (2003) 357–365

JOURNAL OF POWER SOURCES

www.elsevier.com/locate/jpowsour

Small bandwidth measurement of the noise voltage of batteries

D.H.J. Baert*, A.A.K. Vervaet

Department of ELIS, University Gent, Sint-Pietersnieuwstraat 41, B-9000 Gent, Belgium

Received 27 May 2002; received in revised form 5 October 2002; accepted 7 October 2002

Abstract

The purpose of this paper is to measure the very small electrochemical noise voltage (about 10 nV) generated in batteries. The new method presented here is able to realize these measurements of the noise signal in an industrial environment. The technique we developed is based on a small part of the frequency noise spectrum between 3 and 30 Hz. As we will show this seems to offer a good compromise for applications in an industrial environment where a relatively high electrical background noise can be expected to exist. In the proposed measurement setup, we have included the possibility to discriminate between different kinds of noise voltages. This selectivity permits to find indications of different noise generating mechanisms in electrochemical systems, e.g. shot- and burst-noise sources. Measurements confirm the practicability of the proposed measurement setup.

Keywords: Batteries; Noise measurements; Noise mechanisms; State-of-health

1. Introduction

The last decade much attention has been devoted to the determination of the condition of secondary batteries because of the economic impact battery failures can have when they are used in critical applications (e.g. in telecom plants). Existing diagnostic techniques such as conductance or impedance testing give only a partial answer to this problem [1–4]. Electrochemical impedance spectra measurements give more information about the reactions in the battery plates but they are difficult to apply outside a laboratory. Especially, the extended use of hermetically sealed valve-regulated lead–acid batteries (VRLA) has favored the search for new diagnostic methods. The last decade a few researchers have tried to obtain information from the battery plate noise voltage. Since there is a resemblance between the generation of noise voltages in corroding metals and some of the mechanisms that are responsible for battery failure it is reasonable to accept that noise measurements can also be applied for diagnostic purposes.

The subject noise has been studied thoroughly in the 1960s in relation to communication systems [5] and semiconductors [6] but noise measurements have also been used from time to time in electrochemical studies. We will first discuss some of the noise sources that are present in physical and electrochemical systems. Then the requirements for a practical measurement setup will be derived. Finally, some results obtained with the equipment here described will demonstrate the value of the technique we here propose.

Johnson or thermal noise is associated with thermodynamic equilibrium situations. A Johnson noise voltage source shows Poisson distributed abrupt amplitude changes that are the result of the random thermal motion of free electrons that collide with the lattice centers in the conductor (Fig. 1a). The theory developed by Nyquist shows that a real resistor with value R can be represented by an ideal resistor R in series with a voltage noise source e which has a mean square value:

$$\overline{e^2} = 4kTBR \tag{1}$$

where k is the Boltzmann's constant, T the absolute temperature and B is the measurement bandwidth. The nature of this resistor is irrelevant: the Nyquist theorem shows that it can be as well a physical resistor as well as a cause of energy losses in the system which can be represented by a resistor in an electric equivalent circuit. In the frequency domain the noise power density spectrum $4KTR$ is flat and determined by the resistance value R.

Shot noise on the contrary is a Poisson distributed series of charge impulses generated in a non-equilibrium physical process. Such a situation occurs, e.g. when free charge carriers are in a random way generated at an electrode. If these carriers are accelerated in an electric field, the

* Corresponding author.
E-mail address: baert@elis.rug.ac.be (D.H.J. Baert).

0378-7753/02/$ – see front matter
PII: S0378-7753(02)00599-2

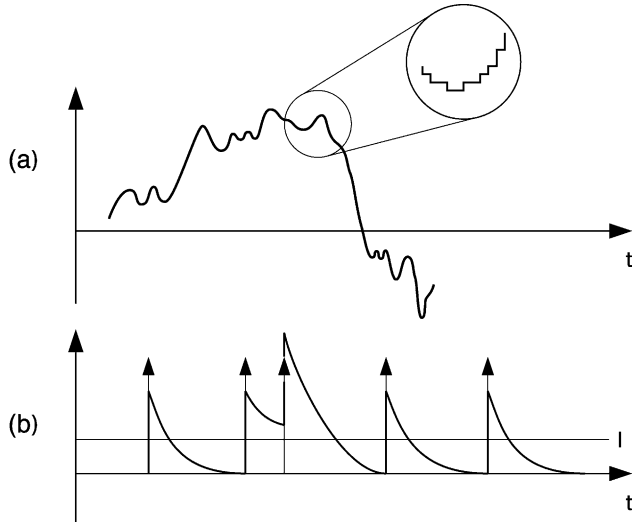

Fig. 1. A Nyquist noise voltage waveform is shown in (a). It looks continuous in practice but it consists of a superposition of random step voltages as shown in the circle. The shot noise impulses in (b) are distorted by the impulse response of the system and form the random sequence of pulses. The arrows are proportional to the charge involved in the phenomenon and I is the average current.

impulses are transformed into Poisson distributed pulses in the electrode current (Fig. 1b). The impulse power density spectrum possesses a dc component and a part flat to very high frequencies, but finally the physical and chemical processes associated with the carrier generation process determine the measurable pulse output spectrum. If the average time between the pulses is short then, in the time domain, this noise can look like a dc current I with stochastic fluctuations i superposed. The mean square value of the current fluctuations is proportional to the dc current:

$$\overline{i^2} = 2qBI \tag{2}$$

where q is the elementary charge. Although all the noise sources from above are due to single events, the large number of events makes the noise appear as a continuously with time varying quantity described by a stochastic process. Therefore, it is possible to attribute a probability density function to the fluctuations. Due to the central limit theorem of statistics this function will be the Gaussian or normal distribution function

$$p_x(x) = \left(\frac{1}{\sigma\sqrt{2\pi}}\right) \mathrm{e}^{-(x-m)^2/2\sigma^2} \tag{3}$$

where m is a mean value and σ^2 is a mean square value. In the case of Schottky noise $m = I$ and $\sigma^2 = \overline{i^2}$.

In general, in electrochemical systems complex electrochemical reactions occur. Tyagai [7] has studied the different ''Faradaic'' sources of noise associated with these reactions using a method developed by Langevin [6]. First, one has to consider the noise that is closely related to the Faradaic impedance of the system near equilibrium and which is in fact Johnson noise. The effective voltage of this noise source thus only depends on the real part of the Faradaic impedance and the absolute temperature. The Faradaic impedance can be determined from the differential equations governing the system. Systems not in equilibrium generate electrochemical or Faradaic noise. Such condition occurs, e.g. during adsorption, diffusion, chemical reactions, random fluctuations of reactant concentrations, ... The noise is introduced into the macroscopic impedance obtained from the differential equations by inserting in these equations fluctuating perturbations, equivalent to the actual noise sources. The determination of the specific form of these noise sources is however not simple. Tyagai uses statistical considerations because this gives the broadest scope of applications. The following is required to apply statistical considerations [7]:

(1) Every slow step of a complex electrode reaction has to be taken into account for calculation of the Faradaic noise. The forward and the backward reactions must be represented by two uncorrelated noise sources.
(2) The activation energy of the reaction must exceed the thermal motion energy of the particles so that a non-equilibrium state exists.
(3) The (measurement) time interval considered must be greater than a single reaction event so that statistical averages can be determined.

Under these conditions the noise sources, which represent the single events of the reaction, are of the shot noise type.

The power density spectrum of the noise that can be measured externally is then calculated via the transfer function from the noise source to the output of the macroscopic impedance network. The noise sources do not explicitly require the presence of charged particles or a net reaction current. Charge carriers exchanged in a reaction suffice. In this case, there exists diffusion, the fluctuations in the active component also produces noise. If a net current flows out of the system, one or more shot noise sources proportional to this current will exist. The charge value of the random shot noise impulses and the average impulse rate depend on a specific electrochemical reaction under consideration. Every electrochemical reaction in the system produces its own impulse sequence and the current pulse response is determined by its reaction kinetics. The measurable noise voltage at the battery connections is a superposition of all these pulse responses.

It is clear that the perception of a shot noise waveform depends on the average impulse rate. If this time interval is large then the pulse shape will be the pulse response of the equivalent electrochemical network to a single impulse. If the individual pulse responses overlap, then the noise current resembles a dc current with fluctuations. Sometimes the pulses occur in bursts, as is the case with some corrosion mechanisms [8].

In batteries noise finds its origin in the complex reaction kinetics and diffusion processes at both electrode surfaces, in the transport of the reactive species in the bulk of the solution [9] and in fluctuations of the ion densities.

For instance, in lead–acid batteries we can see that all interactions of the current carriers (electrons, holes, O^--radicals) during their passage from/to the bulk of a metallic electrode must be considered: solid state reactions [10,11], delay times of the reactions, activation energy, influence of electrical fields, grain boundaries, temperature.

For a battery under charge or discharge the main noise voltage sources will be of shot noise nature since current flows. But, due to the complicated nature of the plate reactions we will detect noise that is the result of numerous different mechanisms. On the other hand, when there is no current flow, some local discharge reactions still remain and are a cause of noise, which can be detected at the battery terminal. A small part of the noise voltage can be attributed to the parasitic reactions associated with grid or connector rod corrosion.

In systems such as batteries and semiconductors a group of noise mechanisms (flicker noise) can be represented by resistance fluctuations [6]. A typical example is the contact resistance between the conducting active mass particles or between grid and active mass. If a current I flows to a resistance R that has fluctuations δR, the mean square value of the voltage over R is

$$\overline{\delta V^2} = I^2 \overline{\delta R^2} \tag{4}$$

This noise source should be dominant at high currents because of the exponent of I. Its power density spectrum is mostly proportional to $1/f$.

Although the noise power density spectrum at the battery connectors can in principle be calculated from the individual electrochemical reactions, this is impossible to work out because of the complexity of the phenomena. In practice we can only measure the total noise density spectrum and thus, no information about the individual sources can be obtained. It has been shown [12] that for reasonable physical events a noise density spectrum has a shape proportional to $1/f^{\alpha}$ with $\alpha = 1$–2. It follows that spectrum measurements cannot provide very much information about specific processes in the battery. On the other hand, it becomes possible to simplify a noise measurement by considering only a small but representative part of the spectrum. From this part, the effective noise (root of mean square) voltage can then be calculated.

2. Battery life time characteristics

The state of a battery is expressed [13] by the state-of-charge (SOC) and the state-of-health (SOH). In contrast with the capacity that can be drawn from a battery, represented by a number, the SOH is a more vague notion. The SOH describes the aging of the battery and allows a prediction of future performance. It is mainly determined by the operational conditions of the battery. If a battery is, e.g. floated at a too high temperature the corrosion rate is very high and failures will occur. The SOC relates to nominal capacity C_N which is determined by a specific discharge time T_N and current I_N so that $C_N = I_N T_N$. If the battery is discharged with I_N and the actual capacity drawn is C_a then the SOC before discharge was $100C_a/C_N$ (%). The capacity C_a however depends on aging and SOH. It is in general accepted that a battery becomes useless when C_a falls below 80% of C_N. On the other hand, if the battery is completely healthy it is possible that C_a is less than C_N because it was not completely charged at the start of the discharge. In this case, a test that predicts the available capacity would be very valuable. The question is what can be expected or not from noise measurements? From the above reasoning the following considerations result:

(1) *Batteries at float*: The gas recombination reaction will mask the state of the plates.
(2) *Batteries at rest*: At equilibrium the noise level should approach a value determined by the Nyquist equation. If this level is too high this indicates that probably a spurious activity takes place in the battery, e.g. a large self-discharge rate.
(3) *Batteries during discharge*: Due to the existence of shot noise and resistance fluctuations we expect to find components in the effective noise voltage proportional to $I^{1/2}$ and I. A number of sudden death failures in VRLA cells can be attributed to corroding connection rods and plates that cause a catastrophic interruption in the current path. In this case. a generalized corrosion and a cracked structure of the rods is often observed. In most cases, however, these cells pass a classic conductance or discharge test. In view of the sensitivity of noise measurements to resistance fluctuations in the conducting path, there is a possibility that these can predict some of the failures when a current flows. It is also expected to find some indication of deteriorating conduction between conducting plate particles when the battery is worn out since this is also accompanied with resistance fluctuations.
(4) The highly doped oxides on the positive plate and the sponge lead on the negative plate are very good conductors [14] whilst the sulfate is an insulator. The noise voltage associated with these materials during transformation will consequently be low. The corrosion layer on both plates formed during formation of the plates is also a very good conductor. The continuous transformation from lead and lead oxide to lead sulfate creates local insulating spots on the conducting skeleton of the plates and in turn this can be associated with resistance fluctuations.
(5) From (2), it appears reasonable to accept that an open-circuit noise voltage will not yield much information about SOC or SOH. However, it is an accepted fact that the SOC can only be determined correctly by a full discharge test. A number of attempts show that at least a 30% discharge is necessary to estimate the available capacity. If such a test could be reduced to say a 15%

discharge, a considerable gain in testing time is possible. We will draw therefore the evolution of noise voltage during the first period of the discharge in order to see if there exists a correlation between SOC and noise voltage behavior.

In the electronic components industry noise measurements are sometimes used for the prediction of device reliability [15]. Especially, the presence of bad connections or welds seems to produce a noise level above the value that is normally associated to the Johnson noise of the resistive parts of the components. In 1974, Euler [16] has experimented with noise measurements on primary batteries. Iverson [8] was the first to apply noise measurements for the study of metal corrosion. Hladky and Dawson reintroduced this technique in 1981 [17] and 1982 [18] and demonstrated the difference between crevice and pit attack of metals in a corroding solution. In 1988 Lehockey et al. [19] applied noise measurements to the study of structural corrosion in battery plates. Roberge et al. [20] studied noise generation during charge in sealed lead–acid cells that were subjected to severe conditions. Lowe et al. [21] proposed a continuous corrosion rate measurement by noise resistance calculation, but the resistance defined has no direct connection to the electrochemical resistances. Recently, Martinet et al. [22] have proposed noise measurements as a means for the detection of overcharging conditions in different types of batteries (Ni–MH, Li-ion). The first attempts by Baert and Vervaet made to evaluate noise measurements were presented in 2001 [23]. The sensitivity of the setup was however not sufficient to demonstrate convincing results. In the setup, we describe below, the sensitivity was increased while at the same time spurious components were considerably attenuated.

3. Experimental noise measurement setup

For a commercial noise measurement system operating in the industrial environment, the following requirements listed are obvious: very high voltage gain amplification factor K, reasonable measurement time, in situ testing of the battery, no need for screening the batteries, immunity to operating equipment near the batteries, expression of the result as a simple and relatively easy to interpret number. The first requirement is due to the large active plate area of batteries with a capacity of 100 Ah or more. Since the local noise sources of large plates tend to cancel, the resulting total noise is very small. In a first approximation, the noise voltage is inversely proportional to the plate area [16]. There is a large difference between the equipment needed for a practical test on VRLA batteries and a setup meant for research purposes. The simplest equipment used in [8,16] for noise measurements consisted of a sensitive root mean square voltmeter. The bandwidth of the voltmeter in [16] extended to 10 kHz. Hladky and Dawson [18] used a computerized setup with a microprocessor voltmeter, a spectrum analyzer and a plotter. The recorded frequency range extended from 1 mHz to 1 Hz. Lehockey et al. [19] measured in a frequency range of 10^{-4} to 10^{-1} Hz with a commercially designed electrochemical noise measuring system (CML Ltd.). The system used by Martinet et al. [22] digitizes the amplified noise signal in a Nicolet oscilloscope and the data are subsequently Fourier transformed in a PC. The frequency range extends from 0.01 to 10 Hz. It is clear that in all these cases a very long measurement time is required with the extremely lower bound of the frequency range. A lowest frequency of 0.1 Hz requires at least several tens of seconds for obtaining a sufficiently stable value of the corresponding spectrum component. Further we notice that only small pieces of an electrode, e.g. 2 cm × 2 cm, were investigated. Only in [22] the tests were performed on complete batteries, but in laboratory conditions. To fulfill the requirement of a reasonable measurement time, the lowest frequency has to be carefully chosen. The lower this frequency, the larger the noise signal becomes since a part of the noise is due to the slow reactions. We found that a 3 dB cut-off frequency of 3–5 Hz for the amplifier frequency curve is suitable since it allows measurement times of the order of a few seconds. Very slow processes such as diffusion, etc. cannot be detected, but these are not of our interest.

The upper pass-band frequency is determined by the presence of mains frequency components and other disturbances. For a 50 Hz grid, a value in the range of 30–40 Hz still allows a very high attenuation of the mains fundamental. The resulting measurement frequency band therefore contains almost one decade of the noise voltage. The final pass band and an additional gain of 100 is obtained by inserting extra low pass and high pass filters after the noise voltage amplifiers. A 50 Hz notch filter and a low pass filter reduce the remaining mains voltage fundamental and harmonic components (Fig. 2). With these precautions the need for magnetic and electric screens around the batteries is avoided and the battery can be tested in situ on the condition that the environmental electric disturbance level has a reasonable magnitude. The last requirement listed rejects the use of complicated frequency analyzers because the results are difficult to interpret.

The low noise measurement circuit here proposed (Fig. 3) has two outputs. Output $Q1$ gives the effective value of the noise voltage and output $Q2$ is a pulse counter result. The band pass filters F1 and F2 (SR650) tailor the output spectrum of the low noise amplifiers A1 and A2 (EG&G). Because of the relatively high noise factor of the amplifiers for low source impedances it was necessary to insert an impedance matching transformer (ratio 1/23) between the battery and the amplifiers (block "Imp. Adapt"). The total gain factor K of the amplifiers and filters amounts to 23×10^7.

In order to calculate the effective battery noise voltage and suppress the influence of amplifier noise a correlation technique described in [24] has been implemented. For this

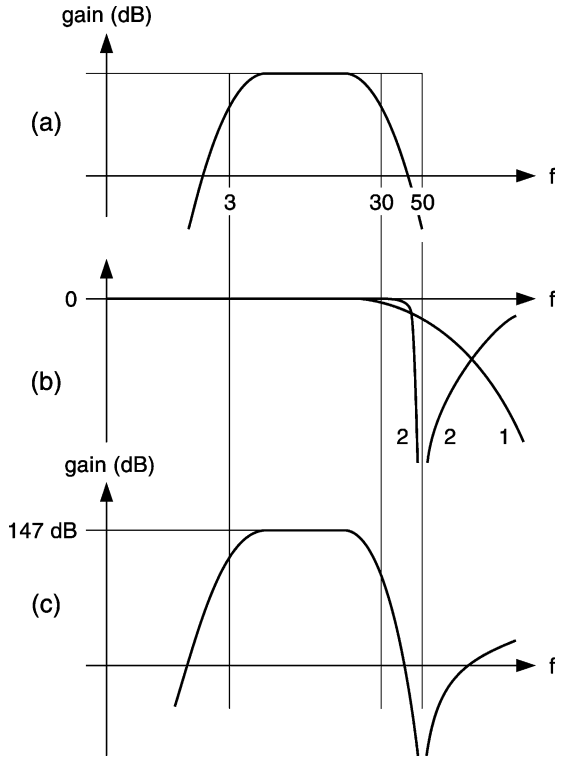

Fig. 2. Frequency response curve of the amplifiers and filters F1 and F2. In (a), we see the response curve of the amplifiers and filters. In (b), the response curves of the low pass filter (1) and the notch filter (2) are shown. Finally, (c) gives the total curve. The gain is expressed in dB (=20 log(gain)) and the frequency scale should be logarithmic.

reason the amplifier chain contains two identical amplifiers and filters (Fig. 3). The blocks multiplier, LP-filter and square-rooter (SQRT) perform an autocorrelation operation and are implemented with a National Instruments ADC board under LabView control. The battery noise signal is amplified in both chains but the outputs are multiplied and the result is

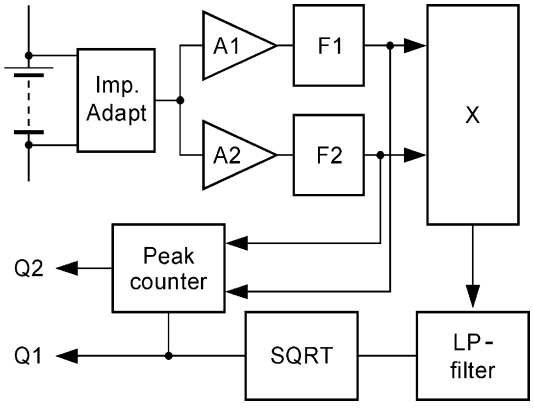

Fig. 3. Noise measurement setup. The amplifiers A1 and A2 are followed by band pass filters F1 and F2. The outputs of the filters are multiplied and the result averaged in the low pass filter LP and after the square root is taken in SQRT the output $Q1$ gives the effective value V_{eff} of the battery noise voltage. This value is used to determine the number of peaks in the noise that exceed a level $\pm 6V_{\text{eff}}$.

averaged in the low pass filter. In this way, the uncorrelated equivalent input voltage noise sources of the amplifiers are eliminated. After taking the square root of the averaged multiplier signal the effective value of the battery noise signal is obtained at the output $Q1$. Care has to be taken in avoiding pickup of mains induced disturbances in the input part of the circuit common to both amplifiers.

The second instrument output $Q2$ is obtained by counting the number of times a certain voltage level determined by output $Q1$ is exceeded at the outputs of the amplifiers. These two outputs are associated with different kinds of noise: an impulsive (large amplitude) part comparable to burst shot noise and a smaller part due to the shot noise sources of the Faradaic equivalent circuit. For a normal probability density distribution of the noise voltage, the probability for finding an instantaneous noise value larger than 3σ is only 0.23%. If we take for the comparator a voltage trip level equal to or larger than six times the effective noise voltage normally no peaks should be detected. On the contrary, if this level is exceeded a number of times this is probably due to burst noise. The indication obtained from the peak counter is however not absolute since we have counted the amplifier outputs separately and these also contain the amplifier noise. Nevertheless, our measurements indicate that useful information can be obtained from this pulse counting method. In particular, if a noise signal increases in amplitude one expects the number of peaks counted to remain the same if there is only noise of one kind present. On the other hand, if burst noise and Gaussian noise are independent, the number of peaks counted should decrease when the effective value increases since this value determines the counter level. If both $Q1$ and $Q2$ increase or decrease at the same time this means different noise mechanisms are at work. It is evident that the statistical deviations in the measurements can be rather large and therefore we calculated averages over a number of points in order to obtain more smoothly varying curves. One measurement takes about 20 s but this can be reduced to 10 s without much influence on the results.

The following batteries were tested: three 6 V nominal 110 Ah Hoppecke OGi VRLA batteries (H1, H2 and H3), a new Cyclon 5 Ah cell, a 15-year-old Cyclon 5 Ah cell and a 5 Ah GP nickel–cadmium cell. Finally, a three-element dry alkaline battery (Varta) was also included in the test.

The Hoppecke batteries were far beyond the 85% end of life capacity limit. The choice of new and old batteries permits to detect differences due to aging phenomena.

4. Measurements and results

All batteries were floated a sufficient long time before the batteries were resistively discharged. Figs. 4–9 give the noise voltages and number of peaks during the discharge. In Figs. 4 and 5a three different states are indicated on the x-axis. The part with the thick line represents the discharge period, the part before this line indicates the start of the

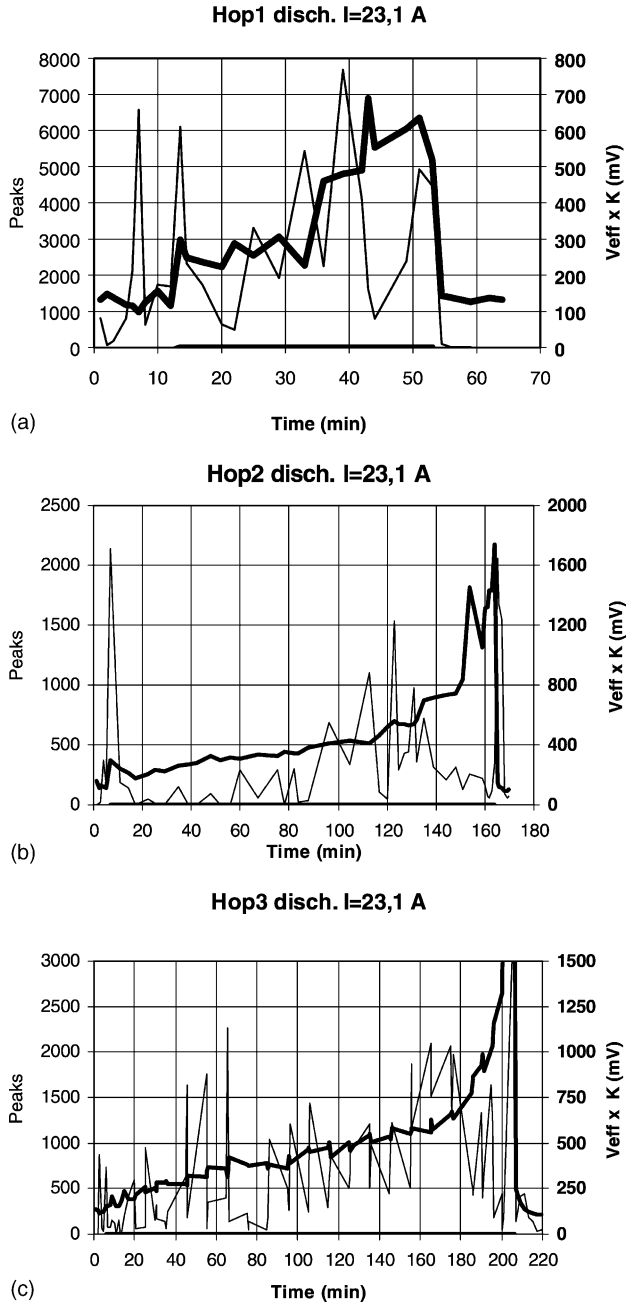

Fig. 4. Noise voltage and peak number for the three Hoppecke batteries during discharge with a current $I = 23.1$ A. The thick line on the x-axis represents the discharge period (a–c).

measurements but without discharge current and finally the part after the thick line shows what happens when the discharge is halted and the battery evolutes to equilibrium. The number of measurement points, shown in Fig. 4, has been reduced somewhat in order to avoid cluttering of the graph. These curves definitely show a generic behavior: the voltage noise level rises continuously during discharge and near the end of the discharge it increases extremely fast. The peak curves have a large dispersion but the general shape of the curves is the same. Near the end of the discharge the peak curves seem to decrease, but this is an artifact due to the

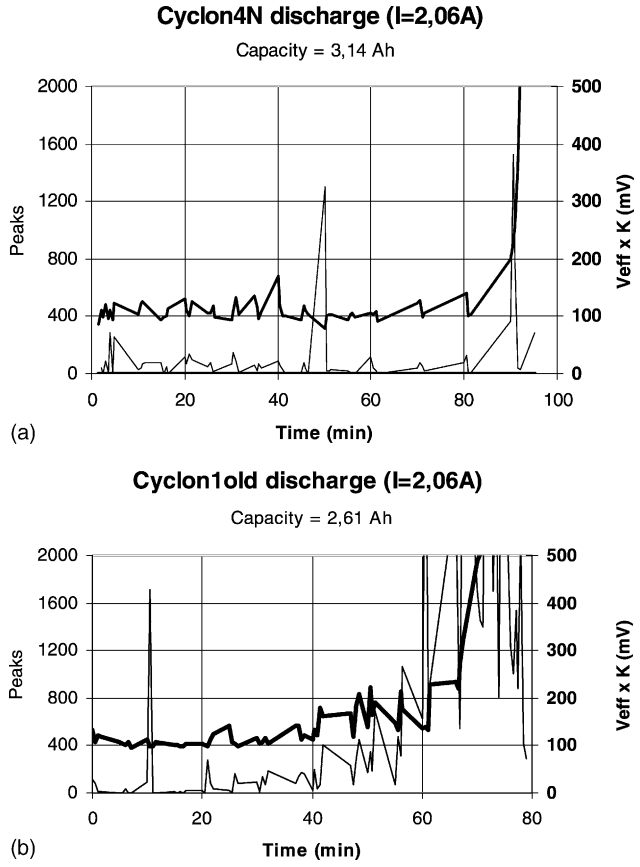

Fig. 5. Noise voltage and peak number for a new (a) and an old Cyclon cell (b).

increasing noise voltage that determines the comparator trip level. This proves that the peak number and noise voltage are more or less independent. The measurements here performed were on battery blocs containing three cells. Because V_{eff} of a bloc is obtained by a quadratic summation of the cell noise voltages, the total noise voltage will normally increase with the square of the number of cells. If this number is not too large then a single noisy cell will considerably influence the total

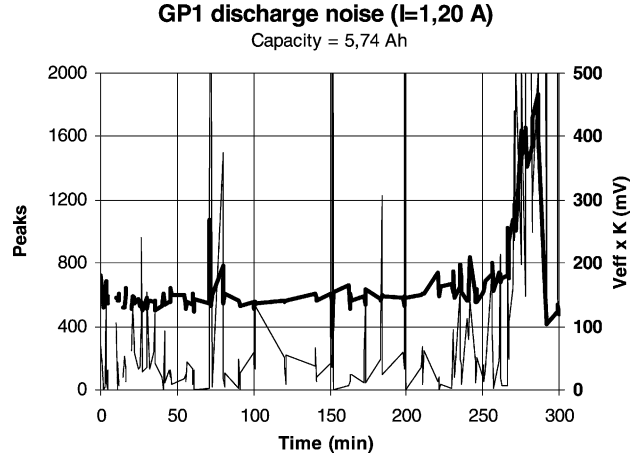

Fig. 6. Noise voltage and peak number for a nickel–cadmium cell GP.

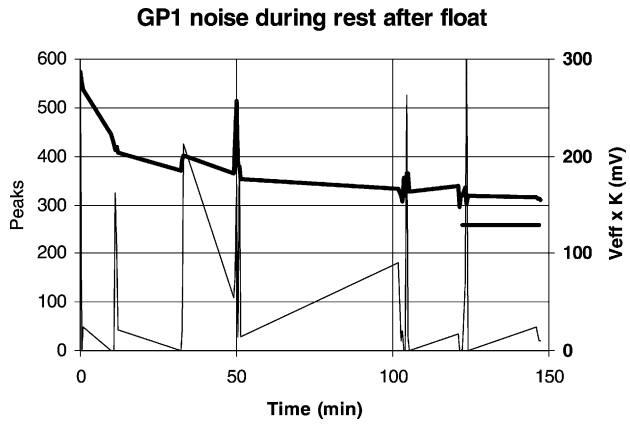

Fig. 7. Restoration of the noise voltage after a period of float for the GP cell.

noise voltage. In most telephone exchange plants, a series connection of blocs of only two or three cells is common.

For the Cyclon cells, we see a relatively flat part of the V_{eff} curve during the first part of the discharge. This is followed by a gradual increase and finally, at the exhaustion of the battery, the noise level becomes very high as is the case for the Hoppecke batteries. A marked difference in behavior between a new (Fig. 5a) and an old Cyclon cell (Fig. 5b) can be seen. This is due to the fact that the increasing part of the curve starts earlier for the old cell than for the new one.

During the discharge of the GP nickel–cadmium cell (Fig. 6) the same generic shape for the V_{eff} curve can be observed. The noise levels of all the cells follow a typical trend immediately after floating when they are left at rest. For example, for the GP cell Fig. 7 gives the noise curve after a float period of 1 month. The voltage noise level drops from about 275 mV (instrument output level) within 10–30 min to a low value, the final value (129 mV) being obtained after several hours.

5. Discussion

When the batteries have been floated for 1 month the noise voltage will be high as occurs for the GP cell (Fig. 7) during the first minutes. This corresponds with the findings of Martinet et al. [22]. The high noise voltage (V_{eff}) after float can be attributed to the presence of oxygen on the positive plate. The corresponding number of peaks is very low and partly this is due to the large V_{eff} that determines the peak level limit.

Hoppecke batteries: There seems to exist a relation between the state-of-health of the battery and the noise voltage: the lower the noise voltage, the higher the final capacity that is obtained. A possible explanation is that the noise voltage is inversely proportional to the active plate area. The worst battery also shows more excess noise probably due to loose contact between conducting particles. The V_{eff} noise curve during discharge consists of two parts:

(1) During the first part, the noise voltage increases almost linearly with time. In particular, if we consider only this part

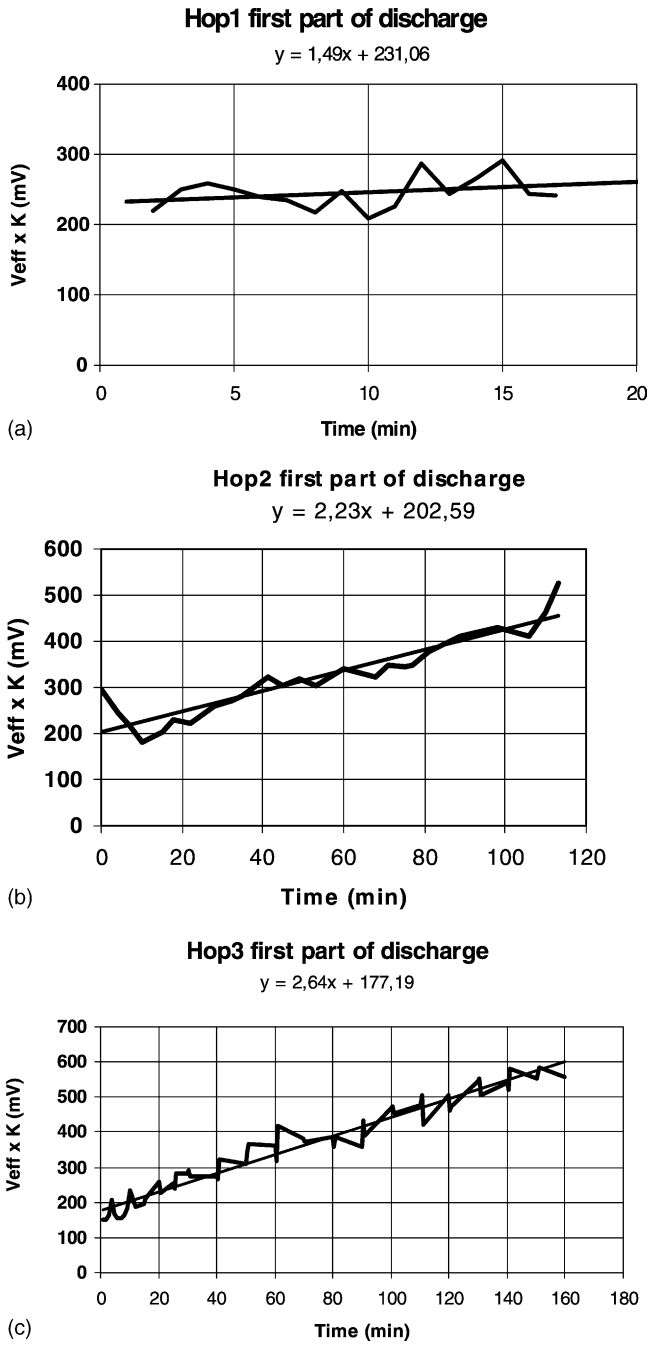

Fig. 8. First part of the discharge noise curve for the Hoppecke batteries. The equations of the trend lines are also given (a–c).

(Fig. 8a–c), we can compare the measurements with the corresponding linear trend line $y = ax + b$. For this graph, we included all the available measurement points and also changed the origin of the time scale so that the start of the discharge coincides with the origin of the thick part on the axis of the Fig. 4. The coefficient a increases with the available capacity which is the largest for the battery in the best SOH. The constant b decreases with the capacity and this indicates that the battery with the best SOH has the lowest initial noise level. Since the discharge current is the

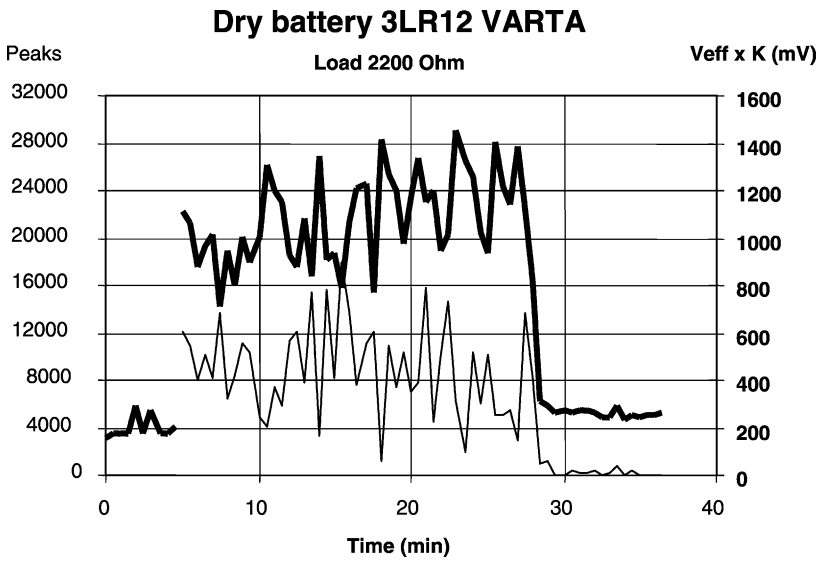

Fig. 9. Noise voltage and peak number for a fresh alkaline dry cell 3LR12. The battery is at rest during the first 5 min and shows very little activity. During the load period (2200 Ω) V_{eff} and the peak number abruptly rises and remains nearly constant. When the load is disconnected both tend slowly to the rest situation.

same during all the tests the differences must be due to the state of the plates, the dominance of some noise sources or to excess noise sources. (2) The second part shows a steep increase of V_{eff} at the end of the discharge and this excess noise can be associated to resistance variations. Following Eq. (4), this noise voltage should in this case be proportional to $I\sqrt{\overline{\delta R^2}}$. Since δR is proportional to the internal resistance of the conductive path of the active plate material its value increases towards the end of discharge. In a first approximation, this part of the resistance is proportional to the active plate area and thus inversely proportional to $1/(1 - t/T_{\text{d}})$ with T_{d} the discharge time. The peak noise curves follow more or less the V_{eff} curves but the most worn out battery (Fig. 4a) shows a very high activity. The fact that the peak noise and V_{eff} curve both rise simultaneously indicates that two different noise sources are observed. The peak number falls at the end of discharge due to the very high value of V_{eff} in this region that determines the comparator trip level.

Cyclon cells and GP cell: The largest difference with the Hoppecke batteries is seen during the first part of the discharge curve that remains flat until about 40 or 65% of the discharge time has elapsed.

Dry cell: Three regions can be distinguished in the V_{eff} curve: the situation at rest, during and after discharge (Fig. 9). The noise voltage and the number of peaks are high and this corresponds with the fact that small plates generate more noise. After the discharge period both quantities slowly recover to a rest value.

6. Conclusions

The results in this article indicate that battery noise can successfully be measured and that it is possible to distinguish between cells in different conditions of wear.

The measurement setup here proposed is capable of determining two noise parameters of a battery, the effective noise voltage and the number of peaks due to burst noise in the voltage wave shape in a time interval. The sensitivity is larger than for former setups due to the use of a two-channel correlation technique. All the requirements we proposed for the measurement on a battery are more or less fulfilled. The setup was used in a normal environment with PCs operating in the neighborhood and without screening the batteries. Statistical variations in the V_{eff} curves of the figures are limited to about 10%. The dispersion on the peak measurements is larger but the trend corresponds to the V_{eff} measurements and our expectations.

Actually, it is possible to derive relative statements from these measurements.

(1) The effective voltage noise levels at rest, 1 h after float, is the almost the same within the group of the three Hoppecke batteries and the group of the two Cyclon cells. However, there is a difference between the rest levels of the Hoppecke batteries, the Cyclon and GP cells.
(2) The effective noise voltage of a battery and the number of peaks occurring during the discharge time give an indication for the SOC and the condition or aging of the battery.
(3) If we consider the three Hoppecke batteries for which we know that they are in a very different state-of-health it is clear that the three trend lines in Fig. 4 give a fair indication of the SOH.
(4) Apparently a short time discharge, say 15% of the nominal discharge time (about 25 min the Hoppecke batteries discharged at 23.1 A), could give some indication of the condition and/or the SOC of a Hoppecke battery.

The measurements here proposed can serve as guidance future research on different kind of batteries in order to evaluate this technique as a diagnostic tool.

References

[1] A.R. Waters, K.R. Bullock, Monitoring the state-of-health of VRLA batteries through Ohmic measurements, in: Proceedings of the International Telecommunications Energy Conference (INTELEC), Session 29-1, 1997.

[2] W.H. Edwards, A.I. Harrison, T.M. Wolstenholme, Conductance measurements in relation to battery state-of-charge, in: Proceedings of the INTELEC, Session 18-3, 1997.

[3] J.M. Hawkins, Some field experience with battery impedance measurement as a useful maintenance tool, in: Proceedings of the INTELEC, 1994, pp. 263–269.

[4] D.C. Cox, R. Perez-Kite, Battery state-of-health monitoring, combining conductance technology with other measurement parameters for real-time battery performance analysis, in: Proceedings of the INTELEC, 2000, pp. 342–347.

[5] W.R. Bennett, Electrical Noise, McGraw-Hill, London, 1960.

[6] A. Van Der Ziel, Fluctuation Phenomena in semi-conductors, Butterworths Scientific Publications, London, 1959.

[7] V.A. Tyagai, Faradaic noise of complex electrochemical reactions, Electrochim. Acta 16 (1971) 1647–1654.

[8] W.P. Iverson, Transient voltage changes produced in corroding metals and alloys, J. Electrochem. Soc., Electrochem. Sci. June (1968) 617–618.

[9] C. Gabrielli, F. Huet, M. Keddam, Noise in electrochemical systems, in: Proceedings of the International Conference on ''Noise in Physical Systems and 1/*f* Noise'', North-Holland, Amsterdam, 1983, pp. 385–388.

[10] D. Pavlov, T. Rochachev, Dependence of the phase composition of the anodic layer on oxygen evolution and anodic corrosion of lead electrode in lead dioxide potential region, Electrochim. Acta 23 (1978) 1237–1242.

[11] D. Pavlov, S. Zanova, G. Papazov, Photo electrochemical properties of the lead electrode during anodic oxidation in sulfuric acid solution, J. Electrochem. Soc. 124 (1977) 1522–1528.

[12] D. Halford, A general mechanical model for $|f|^{\alpha}$ spectral density random noise with special reference to flicker noise $1/|f|$, Proc. IEEE 56 (3) (1968) 251–258.

[13] D. Berndt, Maintenance-Free Batteries, Reasearch Studies Press Ltd., Taunton, Somerset, England, 1994, p. 311.

[14] A. Vervaet, D. Baert, The lead–acid battery: semiconducting properties and Peukert's law, Electrochim. Acta 47 (2002) 3297–3302.

[15] M. Gupta, Applications of electrical noise, Proc. IEEE 63 (7) (1975) 996–1010.

[16] K.J. Euler, Das Rauschen von Elektro-chemischen Stromquellen, ETZ-B 24 (1974) 115–117.

[17] K. Hladky, J.L. Dawson, The measurement of localized corrosion using electrochemical noise, Corrosion Sci. 21 (4) (1981) 317–322.

[18] K. Hladky, J.L. Dawson, The measurement of corrosion using electrochemical 1/*f* noise, Corrosion Sci. 22 (3) (1982) 231–237.

[19] E.M. Lehockey, A.M. Brennenstuhl, G. Palumbo, P. Lin, Electrochemical noise for evaluating susceptibility of lead–acid battery electrodes to intergranular corrosion, Brit. Corrosion J. 33 (1) (1988) 29–36.

[20] P.R. Roberge, R. Beaudoin, G. Verville, J. Smit, Voltage noise measurements on sealed lead–acid batteries, J. Power Sources 27 (1989) 177–186.

[21] A. Lowe, H. Eren, Y.J. Tan, B. Kinsella, S. Bailey, Continuous corrosion rate measurement by noise resistance calculation, IEEE Trans. Instrum. Meas. 50 (5) (2001) 1059–1065.

[22] S. Martinet, R. Durand, P. Ozil, P. Leblanc, P. Blanchard, Application of electrochemical noise analysis to the study of batteries: state-of-charge determination and overcharge detection, J. Power Sources 83 (1999) 93–99.

[23] D. Baert, A. Vervaet, Determination of state-of-health of VRLA batteries by means of noise measurements, in: Proceedings of the International Telecommunications Energy Conference, 2001, pp. 301–312.

[24] How to measure noise that is quieter than your opamp, Princeton Applied Research, Application Note 127, 1974.